Imperial College London

Shape and Topology Optimization of Fluid-Structure-Interaction Problems

Pedro Gomes, Rafael Palacios

4th Annual SU2 Developers Meeting

09/05/2019

Contents

Objective

- A new method to perform concurrent shape (aerodynamic) and topology (structural) optimization of aeroelastic problems.
- Apply it to relatively large-scale problems.

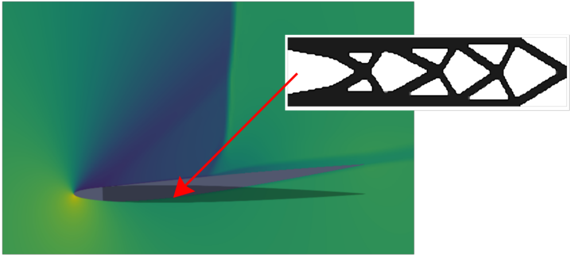

Possible applications

Aircraft range maximization, passive load alleviation, aeroelastic tailoring, additive manufacturing.

State of the Art

Characteristics of existing work

- Minimum-weight-type problems of medium to large size (VERY large for structure only).
- Passive/active load alleviation/augmentation on small scale or 2D problems.
- Dynamic stability of plate-like wings.
- Low fidelity or inviscid fluid modelling.
- Linear elasticity used in most applications.
- Seldom combined with shape optimization.

[Maute and Allen, 2004] Euler + Linear elastic plates, optimum layering, optimum ribs and spars.
[Stanford and Ifju, 2009] Potential flow, passive load alleviation/augmentation.
[James et al. 2014] Potential flow + Linear elastic solid, wing box topology and twist optimization.

Methodology - Structural Topology Optimization

Density approach

- Each element is assigned a density variable ($\rho_{min} \leqslant \rho \leqslant 1$), of which the relevant local material properties are assumed to be a function.
- Intermediate densities are penalized so a discrete solution is obtained (e.g. $E = E_{ref}\,\rho^p$ [Bendsoe, 1989]).
- Special care is needed to avoid numerical issues, filtering the density field with a discrete filter used currently [Sigmund, 2007].

Figure 1: Bad topology, corner contacts

Methodology - Structural Topology Optimization

Topologies obtained with L-BFGS-B and and the exterior penalty method.

Figure 2: 4 by 1 cantilever, 50% material, linear analysis

(a) Topology

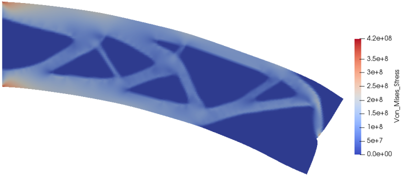

(b) Deformed shape (1:1)

Figure 3: 4 by 1 cantilever, 50% material, nonlinear analysis

Methodology - Linear solvers

A pitfall of density-based topology optimization

Large ill-conditioned linear systems, due to the discretization of empty space, and the stiffness contrast between it and solid regions.

PaStiX (direct sparse solver [Hénon et al. 2002]) integrated in SU2 to allow the solution of "tougher" problems.

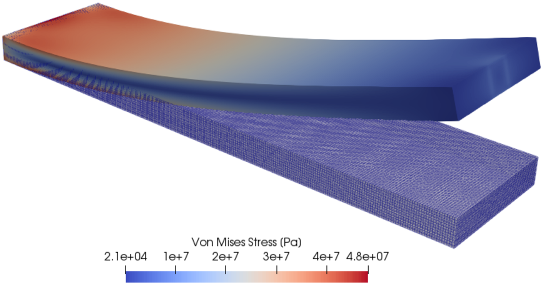

Figure 4: 190k node nonlinear elasticity problem (1:1 scale)

Methodology - Linear solvers - Quick aside

With a linear solver that has no CFL constraints we can investigate the potential convergence rate of the nonlinear and adjoint solvers.

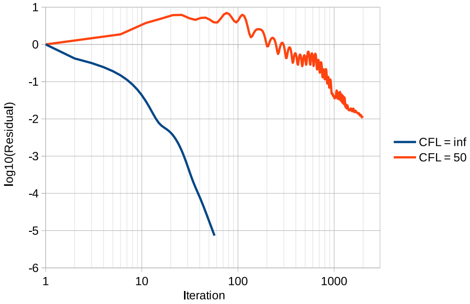

Figure 5: Influence of CFL on the RANS (SST) discrete adjoint solver, NACA0012 80k mesh

Significant speed-up if numerical properties of Jacobians are improved (as this type of linear solver does not scale well in 3D).

Methodology - FSI Coupling Algorithm

Block Gauss-Seidel (BGS) (1) can be slow and sensitive to the relaxation factor (ω), whose optimum value is case dependent.

$$\mathbf{u}_\Gamma^{n+1} = \omega \mathcal{S} \circ \mathcal{F}(\mathbf{u}_\Gamma) + (1-\omega)\mathbf{u}_\Gamma \qquad (1)$$

Interface quasi-Newton methods (IQN) also reduce the problem to finding the interface displacements ($\mathbf{u}_\Gamma$) but state the problem as

$$\mathbf{R}_\Gamma(\mathbf{u}_\Gamma) = \mathcal{S} \circ \mathcal{F}(\mathbf{u}_\Gamma) - \mathbf{u}_\Gamma = \mathbf{r} = \mathbf{u}_\Gamma^* - \mathbf{u}_\Gamma = \mathbf{0} \qquad (2)$$

and solve it iteratively via

$$\mathbf{u}_\Gamma^{n+1} = \mathbf{u}_\Gamma + \tilde{\mathbf{r}}_u^{-1}(-\mathbf{r}) \qquad (3)$$

Ways of obtaining $\tilde{\mathbf{r}}_u^{-1}(-\mathbf{r})$: Matrix-free Krylov, Rank-1 updates or LS approximations.

Methodology - FSI Coupling Algorithm

IQN-ILS (the essence)

At each iteration compute the linear combination of past residuals ($\mathbf{r}$) that tries to minimize the next one (set $\mathbf{u}_\Gamma$ for that iteration as the same combination of past $\mathbf{u}_\Gamma^*$).

Results

Typically 1.5 times faster than BGS. No need for relaxation. But less robust against poor convergence of subproblems.

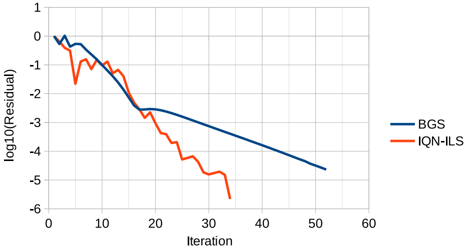

Figure 6: FSI convergence history

Methodology - FSI Coupling Algorithm

What about the FSI adjoint?

The coupled adjoint equations are obtained by considering the block nature of the Jacobian, induced by the three-field partitioned FSI approach, that is

$$\bar{\mathbf{x}} = \mathcal{J}_x^T + \mathcal{G}_x^T \bar{\mathbf{x}} \equiv \begin{pmatrix} \bar{\mathbf{w}} \\ \bar{\mathbf{u}} \\ \bar{\mathbf{z}} \end{pmatrix} = \begin{pmatrix} \mathcal{J}_w^T \\ \mathcal{J}_u^T \\ \mathcal{J}_z^T \end{pmatrix} + \begin{bmatrix} \mathcal{F}_w & \mathbf{0} & \mathcal{F}_z \\ \mathcal{S}_w & \mathcal{S}_u & \mathcal{S}_z \\ \mathbf{0} & \mathcal{M}_u & \mathbf{0} \end{bmatrix}^T \begin{pmatrix} \bar{\mathbf{w}} \\ \bar{\mathbf{u}} \\ \bar{\mathbf{z}} \end{pmatrix}$$

The mesh deformation ($\mathcal{M}$) is designed such that

$$\mathcal{M}_u = 0 \ \forall \ \mathbf{u} \notin \Gamma \rightarrow \mathcal{M}_u^T \bar{\mathbf{z}} = \begin{pmatrix} \mathbf{0} \\ \bar{\mathbf{u}}_\Gamma \end{pmatrix}$$

which allows the adjoint interface problem to be written as

$$\mathbf{R}_\Gamma(\bar{\mathbf{u}}_\Gamma) = \overline{\mathbf{M}} \circ \overline{\mathbf{F}} \circ \overline{\mathbf{S}}(\bar{\mathbf{u}}_\Gamma) - \bar{\mathbf{u}}_\Gamma = \mathbf{0} \qquad (4)$$

Methodology - Shape Optimization of FSI

Verification of shape derivatives (free form deformation box) for FSI cases.

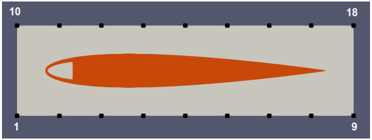

Figure 7: Geometry and control points

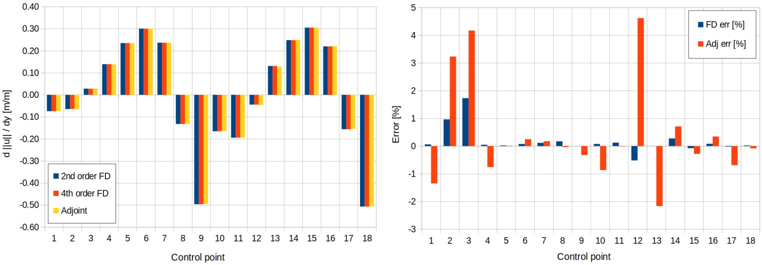

Figure 8: Derivatives and error estimates

Preliminary Results - Shape Optimization of FSI

Optimization problem

Area ($A \geqslant A_0$), lift ($c_l = 0.5$), and deformation ($\delta_{TE} \leqslant \delta_{max}$) constrained, drag minimization. Constraints at low Mach number (0.25), objective at high (0.75).

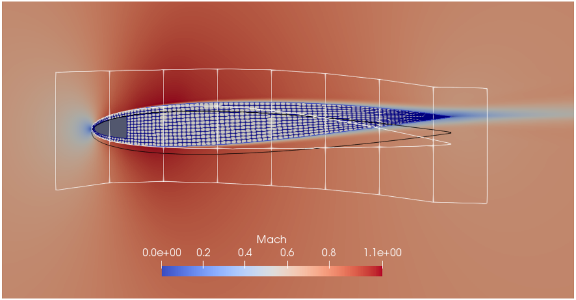

Figure 9: Parameterization

Preliminary Results - Shape Optimization of FSI

Table 1: Shape optimization results

δ_{max}	$\mathbf{c_d^{0.75M}}$	$c_l^{0.75M}$	$c_d^{0.25M}$
10.0 mm	**0.008582**	0.07554	0.01117
6.0 mm	**0.008766**	0.1477	0.01128

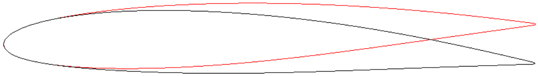

Figure 10: Trailing edge displacement constrained to 10mm

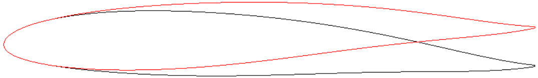

Figure 11: Trailing edge displacement constrained to 6mm

Preliminary Results - Topology Optimization of FSI

Fixed external shape of the 6 mm case, elasticity modulus doubled, weighted objective (80% drag, 20% mass).

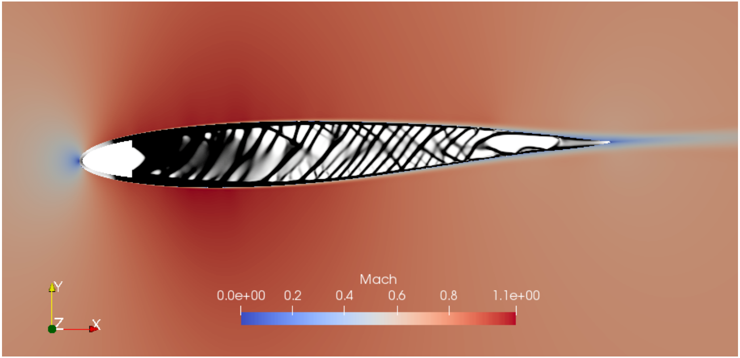

Figure 12: Optimized topology

Preliminary Results - Topology Optimization of FSI

Table 2: Topology optimization results

$\mathbf{c_d^{0.75M}}$	$c_l^{0.75M}$	$c_d^{0.25M}$
0.008606 (-1.8%)	0.04126	0.01194 (+5.9%)

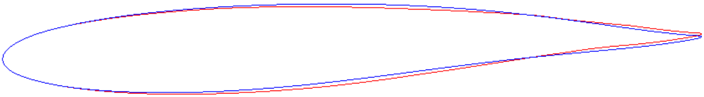

Figure 13: Shape, Topology ∘ Shape

Drag is reduced but topology is not discrete and drag at low Mach increases (as it is not part of the weighted objective).

Summary, Challenges, Future Work

Summary

- Structural topology optimization functionality.
- Less parameter sensitive FSI (and a bit faster).
- Some improvements to linear solvers (hopefully more to come).

Challenges

- Encouraging solid-void topologies (problem definition).
- Dealing with extremes where the structure buckles.
- Computational expense.

Future Work

- Concurrent shape and topology optimization.
- Improve scalability/speed of methods to make 3D possible.